PHYSICAL REVIEW D **86,** 114013 (2012)

Line shape of $\psi(3770)$ in $e^+e^- \to D\bar{D}$

N. N. Achasov* and G. N. Shestakov†

Laboratory of Theoretical Physics, S. L. Sobolev Institute for Mathematics, 630090 Novosibirsk, Russia

(Received 21 August 2012; revised manuscript received 20 November 2012; published 7 December 2012)

Interference phenomena observed in the $\psi(3770)$ resonance region in the reactions $e^+e^- \to D\bar{D}$ are analyzed. To avoid ambiguities in the determination of the $\psi(3770)$ resonance parameters, when analyzing data between the $D\bar{D}$ and $D\bar{D}\pi$ thresholds, the amplitudes satisfying the elastic unitarity requirement should be used. In the lack of information on the P wave of $D\bar{D}$ elastic scattering, the $\psi(3770)$ parameters, determined by fitting the $e^+e^- \to D\bar{D}$ data, can essentially depend on the model used for the total contribution of the resonance and background. The selection of the models can be toughened by comparing their predictions with the relevant data on the shape of the $\psi(3770)$ peak in the non-$D\bar{D}$ channels $e^+e^- \to \gamma\chi_{c0}$, $J/\psi\eta$, $\phi\eta$, etc.

DOI: 10.1103/PhysRevD.86.114013 PACS numbers: 13.20.Gd, 13.25.Gv, 13.40.Gp, 13.66.Jn

I. INTRODUCTION

The resonance $\psi(3770)$ was investigated in the reactions $e^+e^- \to D\bar{D}$ by the MARK-I [1,2], DELCO [3], MARK-II [4], BES [5–13], CLEO [14–16], *BABAR* [17,18], Belle [19], and KEDR [20–23] Collaborations. With increasing accuracy of measurements, there appeared indications on an unusual shape of the $\psi(3770)$ peak, i.e., on possible interference phenomena in its region [8,9,11–13,17–26]. Recently, the KEDR Collaboration noted [21–23] that the parameters of the $\psi(3770)$ resonance become distinctly different from those quoted by the Particle Data Group in the preceding reviews (see, for example, Ref. [27]) if the data analysis takes into account the interference between the $\psi(3770)$ production amplitude and the nonresonant $D\bar{D}$ production one. In Refs. [22,23], two very different solutions for the interfering resonance and background amplitudes were obtained [28]. These solutions lead to the same energy dependence of the cross section and are indistinguishable by the χ^2 criterion. Ambiguities of this type in the interfering resonances parameters determination were found in Ref. [29].

CLEO-c has now accumulated about 818 pb^{-1} [30] and BES III about 2.9 fb^{-1} [31] integrated luminosity on the $\psi(3770)$ peak for open charm physics investigations. Therefore, from CLEO-c and BES III, one can also expect new data with very high statistics on the shape of the $\psi(3770)$ resonance. In this regard, we believe it is timely to discuss some dangers which are hidden in the commonly used schemes for the description of the $\psi(3770)$ peak.

Section II shows that the most precise current data on the $e^+e^- \to D\bar{D}$ reaction cross section in the $\psi(3770)$ region are hard to describe with a single $\psi(3770)$ resonance. In Sec. III, simple models for the isoscalar part of the D meson electromagnetic form factor, F_D^0, which determines the amplitude $e^+e^- \to D\bar{D}$ in the $\psi(3770)$ resonance region, are constructed. The models take into account interference between the resonance and background contributions and yield good descriptions of the data. The form factor F_D^0 is constructed in such a way as to guarantee at least at the model level the elastic unitarity requirement. Information on the P wave of $D\bar{D}$ elastic scattering could be a great help in constructing the D meson electromagnetic form factor. However, such information is not available. Therefore, it is reasonable that the $\psi(3770)$ resonance parameters, derived from fitting the $e^+e^- \to D\bar{D}$ data, can essentially depend on the model used for the sum contribution of the resonance and background. Section IV shows that the selection of the models can be significantly toughened by comparing their predictions with the relevant data on the shape of the $\psi(3770)$ peak in the non-$D\bar{D}$ channels, such as $e^+e^- \to \gamma\chi_{c0}$, $J/\psi\eta$, $\phi\eta$, etc. The results of our analysis are briefly formulated in Sec. V. A comment concerning the ambiguity of the fitting solutions found in Refs. [22,23,29] is given in the Appendix.

II. THE $\psi(3770)$ RESONANCE IN $e^+e^- \to D\bar{D}$

Figure 1 shows the data for the sum of the $e^+e^- \to D^0\bar{D}^0$ and $e^+e^- \to D^+D^-$ reaction cross sections in the $\psi(3770)$ region, $\sigma(e^+e^- \to D\bar{D})$, obtained by BES [8,9] (68 points in the $\sqrt{s}$ region from 3.645 to 3.872 GeV), CLEO [16] (1 point at $\sqrt{s} = 3.774$ GeV), *BABAR* [17,18] (15 points for 3.73 GeV $< \sqrt{s} <$ 3.89 GeV), and Belle [19] (9 points for 3.73 GeV $< \sqrt{s} <$ 3.89 GeV). Here $\sqrt{s}$ is the energy in the $D\bar{D}$ center-of-mass system. This is the most detailed and accurate current data. It is clear, however, that further improvement of the data and matching the results from different groups are required [32].

Note that the BES Collaboration [8,9] measured, in the region up to the $D\bar{D}^*$ threshold (≈ 3.872 GeV), the quantity $R(s) = \sigma(e^+e^- \to \text{hadrons})/\sigma(e^+e^- \to \mu^+\mu^-)$ [where $\sigma(e^+e^- \to \mu^+\mu^-) = 4\pi\alpha^2/3s$ and $\alpha = 1/137$]. The $D\bar{D}$ events were not specially identified. The BES

*achasov@math.nsc.ru
†shestako@math.nsc.ru

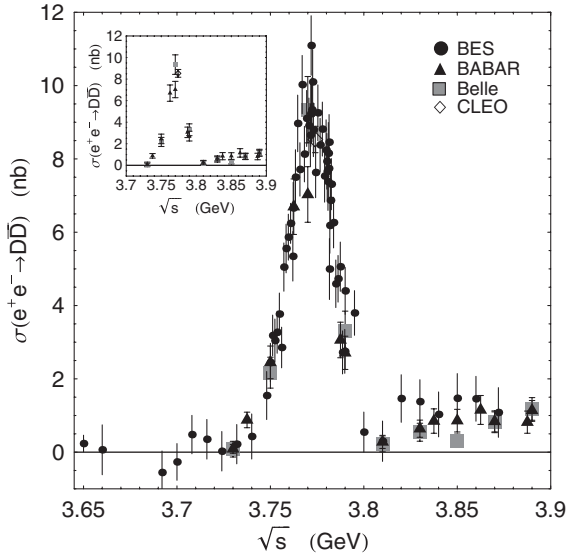

FIG. 1. The data from BES [8,9], CLEO [16], *BABAR* [17,18], and Belle [19] for $\sigma(e^+e^- \to D\bar{D})$. For clarity, the inset shows only the points from CLEO [16], *BABAR* [17,18], and Belle [19].

points shown in Fig. 1 correspond to the cross section $(4\pi\alpha^2/3s)[R(s) - R_{uds}]$, where $R_{uds} = 2.121$ [9] describes the background from the light hadron production. This cross section gives a good estimate for $\sigma(e^+e^- \to D\bar{D})$ in the $\psi(3770)$ region, because it is expected that the decay width of the $c\bar{c}$ state $\psi(3770)$ (or states) into the non-$D\bar{D}$ modes must be comparable with the decay width of the $\psi(2S)$ resonance located under the open charm production threshold. Hence, the ratio $B(\psi(3770) \to \text{non-}D\bar{D})/B(\psi(3770) \to D\bar{D})$ must be small owing to the large total width of the $\psi(3770)$. This is confirmed by experiment [28,33].

The measured $D\bar{D}$ mass spectrum [9,17–19] has the following features. First, the right side of the $\psi(3770)$ peak turns out to be more steep than its left side. Second, there is a deep dip near 3.81 GeV in the mass distribution (in fact, the cross section dips to zero near this point). These features are hard to describe with the help of a single $\psi(3770)$ resonance contribution.

In most experimental works, the $e^+e^- \to D\bar{D}$ cross section caused by the $\psi(3770)$ resonance production was described with minor modifications by the following formula [below, for short $\psi(3770)$ is also denoted as ψ'']:

$$\sigma_{\psi''}(e^+e^- \to D\bar{D}) = \frac{12\pi\Gamma_{\psi''e^+e^-}\Gamma_{\psi''D\bar{D}}(s)}{(m_{\psi''}^2 - s)^2 + (m_{\psi''}\Gamma^{\rm tot}_{\psi''}(s))^2}, \quad (1)$$

where $m_{\psi''}$ is the mass, $\Gamma_{\psi''e^+e^-}$ the e^+e^- decay width, $\Gamma_{\psi''D\bar{D}}(s)$ the $D\bar{D}$ decay width, and $\Gamma^{\rm tot}_{\psi''}(s)$ the total decay width of the resonance. The energy-dependent width $\Gamma_{\psi''D\bar{D}}(s)$ was taken in the form

$$\Gamma_{\psi''D\bar{D}}(s) = G^2_{\psi''}\left(\frac{p_0^3(s)}{1 + r^2p_0^2(s)} + \frac{p_+^3(s)}{1 + r^2p_+^2(s)}\right), \quad (2)$$

where $p_0(s) = \sqrt{s/4 - m^2_{D^0}}$ and $p_+(s) = \sqrt{s/4 - m^2_{D^+}}$ are the D^0 and D^+ momenta, respectively, r is the $D\bar{D}$ interaction radius [34], and $G_{\psi''}$ is the coupling constant of the ψ'' to $D\bar{D}$. Because the $\psi'' \to D\bar{D}$ decay is dominant [28], we put in Eq. (1) $\Gamma^{\rm tot}_{\psi''}(s) = \Gamma_{\psi''D\bar{D}}(s)$. This simplification is not essential for our analysis.

The dashed and solid curves in Fig. 2 show the fits to the data in the region 3.72 GeV $< \sqrt{s} <$ 3.9 GeV (87 points) with the use of Eqs. (1) and (2) at $r = 0$, and 100 GeV^{-1} respectively. In the inset in this figure, the quantity χ^2, characterizing the goodness of fit, is shown as a function of r. As r increases from 0 approximately to 15 GeV^{-1} ($\approx$3 fm), the χ^2 value sharply decreases and then, with r increasing, remains practically unchanged. Such a behavior of χ^2 leaves the parameter r very uncertain. Of course, too large values of r hardly have any physical means [35]. Owing to the parameter r in $\Gamma_{\psi''D\bar{D}}(s)$, one succeeds in raising the left side of the $\psi(3770)$ peak and lowering its right side. In fact, all existing data require such a deformation of the ψ'' peak. However, as is seen from Fig. 2, a dip near 3.81 GeV cannot be explained by varying r. The obtained very unsatisfactory χ^2 values (for the dashed and solid curves in Fig. 2, $\chi^2/n\text{d.o.f.} \approx 413/84 \approx 4.9$ and $248/83 \approx 3$, respectively) are due to both notable differences between the data from different groups and the existence of the dip in the $D\bar{D}$ mass spectrum (for example, for the solid curve in Fig. 2, the points at $\sqrt{s} = 3.8$ and 3.81 GeV yield $\chi^2 \approx 81$). In order to qualitatively improve the data description in the ψ'' resonance region, in particular, to explain a dip near 3.81 GeV, it is necessary to take into account the interference between the resonant and nonresonant $D\bar{D}$ production.

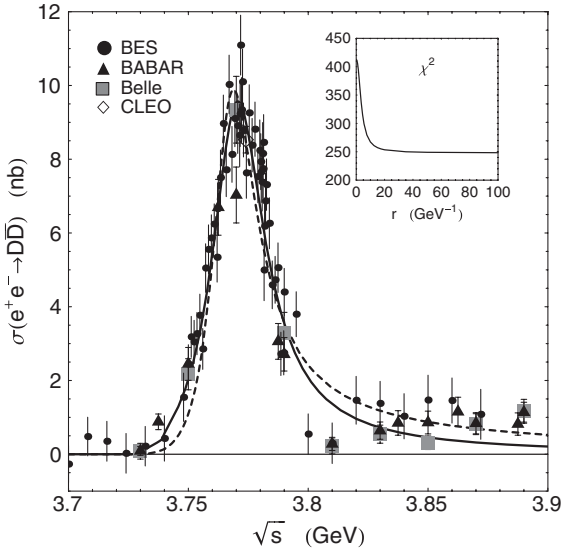

FIG. 2. The results of the fit using Eqs. (1) and (2). The illustration of the $\psi(3770)$ resonance shape dependence on the parameter r. See the text for details.

III. THE D MESON ELECTROMAGNETIC FORM FACTOR

A. Unitarity requirement

In constructing the model describing the process $e^+e^- \to D\bar{D}$, one must keep in mind that we investigate the D meson electromagnetic form factor, the phase of which in the elastic region is completely fixed by the unitarity condition (or the Watson theorem of final-state interaction). Experiment clearly indicates that we deal with the resonant scattering of D mesons. Really, there is the ψ'' resonance between the $D\bar{D}$ and $D\bar{D}^*$ thresholds ($2m_D \approx 3.739$ GeV and $m_D + m_{D^*} \approx 3.872$ GeV), which in a good approximation can be considered as an elastic one, because it has no appreciable non-$D\bar{D}$ decays [28]. Usually, such scattering is described as resonance scattering with an elastic background—see, for example, Ref. [37]—i.e., the corresponding strong amplitude T^I_J with the definite isospin I and spin J (in our case, it is the $D\bar{D}$ scattering amplitude T^0_1) is given by [38]

$$T^0_1 = e^{i\delta^0_1}\sin\delta^0_1 = \frac{e^{2i\delta_{\rm bg}} - 1}{2i} + e^{2i\delta_{\rm bg}}T_{\rm res}, \tag{3}$$

where $\delta^0_1 = \delta_{\rm bg} + \delta_{\rm res}$ is the scattering phase, $\delta_{\rm bg}$ is the elastic background phase (or the phase of potential scattering), and $\delta_{\rm res}$ is the phase of the resonance amplitude $T_{\rm res}$ (in the simplest parametrization $T_{\rm res} = \frac{\Gamma/2}{M-E-i\Gamma/2}$). Then, according to the unitarity condition ${\rm Im}F^0_D = F^0_D T^{0*}_1$, the D meson isoscalar form factor F^0_D [39] has the form in the elastic region

$$F^0_D = e^{i\delta^0_1}G^0_D = e^{i(\delta_{\rm bg}+\delta_{\rm res})}G^0_D, \tag{4}$$

where G^0_D is the real function of energy. A similar representation of the amplitude $e^+e^- \to D\bar{D}$ used for the data description guarantees the unitarity requirement on the model level. The sum of the $e^+e^- \to D\bar{D}$ reaction cross sections is expressed in terms of F^0_D in the following way:

$$\sigma^{D\bar{D}}(s) = \frac{8\pi\alpha^2}{3s^{5/2}}|F^0_D(s)|^2[p^3_0(s) + p^3_+(s)]. \tag{5}$$

B. A simplest model for F^0_D: Resonance plus background

To understand how the form factor and strong amplitude can be constructed to satisfy the unitarity requirement, the easiest way to use the field-theory model shown in Fig. 3 and write

$$T^0_1(s) = \frac{\mathcal{T}^0_1(s)}{1 - i\mathcal{T}^0_1(s)}, \tag{6}$$

$$F^0_D(s) = \frac{f^0_D(s)}{1 - i\mathcal{T}^0_1(s)}, \tag{7}$$

where

$$\mathcal{T}^0_1(s) = \nu(s)t^0_1(s), \tag{8}$$

$$\nu(s) = [p^3_0(s) + p^3_+(s)]/\sqrt{s}, \tag{9}$$

$$t^0_1(s) = \lambda + \frac{1}{6\pi}\frac{g^2_{\psi''D\bar{D}}}{m^2_{\psi''} - s}, \tag{10}$$

$$f^0_D(s) = \lambda_\gamma + \frac{g_{\psi''\gamma}g_{\psi''D\bar{D}}}{m^2_{\psi''} - s}. \tag{11}$$

Graphically, the amplitude $T^0_1(s)$ and the form factor $F^0_D(s)$ defined in Eqs. (6) and (7) corresponds to the infinite chains of the diagrams in Fig. 3 with the real D and $\bar{D}$ mesons in the intermediate states. The amplitude t^0_1 and the form factor f^0_D defined in Eqs. (10) and (11) specify the structure of primary mechanisms included in the model to describe the ψ'' resonance region. The constants λ and λ_γ effectively take into account background (nonresonant in the ψ'' region) contributions to the strong amplitude and form factor, respectively, and the constants $g_{\psi''D\bar{D}}$ and $g_{\psi''\gamma}$ describe couplings of the ψ'' to the $D\bar{D}$ and virtual γ quantum, respectively. The requirement of the unitarity condition is fulfilled in the model under consideration: The phase of the form factor $F^0_D(s)$ is defined by the phase of the amplitude $T^0_1(s)$. This phase has the dynamical origin.

The physical content of Eqs. (6) and (7) will become more clear if they are rewritten in the form of Eqs. (3) and (4), respectively. As a result, we obtain the following expressions for the background and resonance components of $T^0_1(s)$:

$$T_{\rm bg} = \frac{e^{2i\delta_{\rm bg}(s)} - 1}{2i} = \frac{\nu(s)\lambda}{1 - i\nu(s)\lambda}, \tag{12}$$

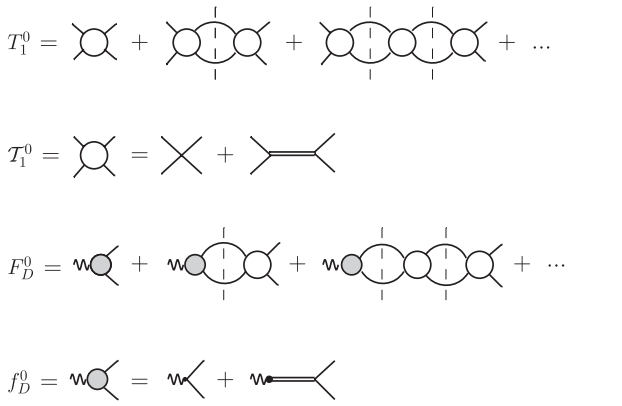

FIG. 3. The graphical representation of the strong $D\bar{D}$ scattering amplitude T^0_1 and the D meson electromagnetic form factor F^0_D. The vertical dashed lines show that the D and $\bar{D}$ mesons in the loops are on the mass shell. Diagrams corresponding to the amplitude $\mathcal{T}^0_1$ and the form factor f^0_D show the structure of primary mechanisms included in the model to describe the ψ'' resonance region.

$$T_{\rm res} = \frac{\sqrt{s}\Gamma_{\psi''D\bar{D}}(s)}{M^2_{\psi''} - s + {\rm Re}\Pi_{\psi''}(M^2_{\psi''}) - \Pi_{\psi''}(s)}, \quad (13)$$

where

$${\rm Im}\,\Pi_{\psi''}(s) = \sqrt{s}\Gamma_{\psi''D\bar{D}}(s) = \frac{\tilde{g}^2_{\psi''D\bar{D}}(s)}{6\pi}\nu(s), \quad (14)$$

$${\rm Re}\,\Pi_{\psi''}(s) = -\lambda\frac{\tilde{g}^2_{\psi''D\bar{D}}(s)}{6\pi}\nu(s)^2, \quad (15)$$

$$M^2_{\psi''} = m^2_{\psi''} - {\rm Re}\Pi_{\psi''}(M^2_{\psi''}), \quad (16)$$

$$\tilde{g}_{\psi''D\bar{D}}(s) = \frac{g_{\psi''D\bar{D}}}{|1 - i\nu(s)\lambda|}. \quad (17)$$

For $F^0_D(s)$ we obtain

$$F^0_D(s) = e^{i\delta^0_1(s)}\frac{(m^2_{\psi''} - s)\tilde{\lambda}_\gamma(s) + g_{\psi''\gamma}\tilde{g}_{\psi''D\bar{D}}(s)}{|M^2_{\psi''} - s + {\rm Re}\Pi_{\psi''}(M^2_{\psi''}) - \Pi_{\psi''}(s)|}, \quad (18)$$

where $\delta^0_1(s) = \delta_{\rm bg}(s) + \delta_{\rm res}(s)$ [$\delta_{\rm bg}(s)$ and $\delta_{\rm res}(s)$ are the phases of the amplitudes (12) and (13), respectively] and

$$\tilde{\lambda}_\gamma(s) = \frac{\lambda_\gamma}{|1 - i\nu(s)\lambda|}. \quad (19)$$

Thus $F^0_D(s)$ incorporates the resonance contribution (proportional to $g_{\psi''\gamma}$) modified (dressed) by the strong background [40] and the proper background contribution (proportional to λ_γ) modified by the strong resonance and background final-state interactions. The numerator in Eq. (18) is proportional to the first-degree polynomial in s, $\lambda_\gamma(m^2_{\psi''} - s) + g_{\psi''\gamma}g_{\psi''D\bar{D}}$, with real coefficients. This ensured that the dip in $\sigma(e^+e^- \to D\bar{D})$ near 3.81 GeV can be explained by the zero in $F^0_D(s)$, caused by compensation between the ψ'' resonance and background contributions. Note that the presence of the zero in $F^0_D(s)$ is in qualitative agreement with the coupled-channel model prediction [41].

As is seen from Fig. 4, the constructed model for $F^0_D(s)$ yields a quite reasonable description of the data (here $\chi^2/n{\rm d.o.f.} \approx 123/82 \approx 1.5$, which is much better than the above $\chi^2/n{\rm d.o.f.}$ values for the fits shown in Fig. 2). For the solid curve in Fig. 4, the cross section at the maximum (located at $\sqrt{s} = \sqrt{s_{\rm max}} \approx 3.773$ GeV) $\sigma_{\rm max} \approx 9.13$ nb, the full width of the peak at its half maximum $\Gamma_{\rm hmax} \approx 29.7$ MeV, and the effective electron width of the resonance structure $\Gamma^{\rm eff}_{e^+e^-} = s_{\rm max}\sigma_{\rm max}\Gamma_{\rm hmax}/(12\pi) \approx 0.263$ keV. These characteristics of the observed peak are in close agreement with the values of the mass (≈ 3.773 GeV), the total width (≈ 27.2 MeV), and the electron partial width (≈ 0.262 keV) which are quoted by the Particle Data Group [28] as the averaged individual characteristics of the ψ'' resonance. However, the peak

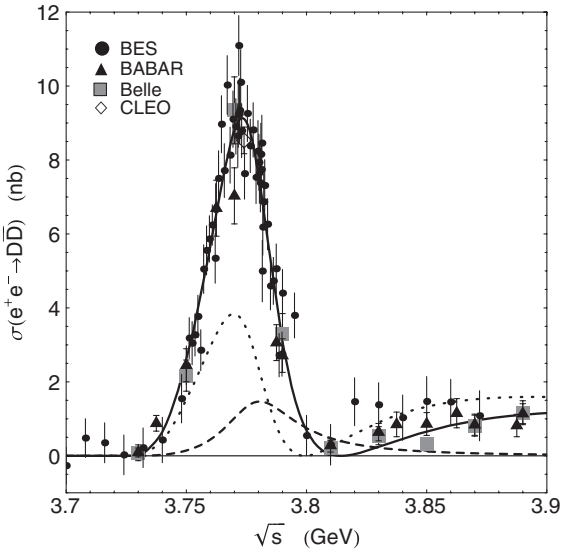

FIG. 4. The resonance plus background model. The solid curve is the result of fitting the data with the use of Eqs. (5) and (18). The dashed curve shows the contribution from the ψ'' resonance production ($\sim g_{\psi''\gamma}$ in F^0_D), and the dotted curve shows the contribution from the background production ($\sim\lambda_\gamma$ in F^0_D) modified by the strong resonance and background final-state interactions.

(in its line shape there is a zero at $\sqrt{s} \approx 3.814$ GeV) does not correspond to a solitary resonance. Therefore, it is reasonable that the model parameters for ψ'' differ from the effective parameters of the visible peak. Let us present the corresponding numbers.

The curves in Fig. 4 correspond to the following values of the fitted parameters: $m_{\psi''} = 3.799$ GeV, $g_{\psi''D\bar{D}} = \pm 19.35$, $g_{\psi''\gamma} = \pm 0.1483$ GeV^2, $\lambda = -30.35$ GeV^{-2}, and $\lambda_\gamma = \pm 25.07$ [if $\lambda_\gamma > 0 (< 0)$, then $g_{\psi''\gamma}g_{\psi''D\bar{D}} > 0 (< 0)$; see Eq. (18)]. As the individual characteristics of the ψ'' resonance, one can take the quantities dressed (renormalized) by the background contributions [see Eqs. (13)–(17)]: $M_{\psi''} = 3.784$ GeV, $\Gamma^{\rm ren}_{\psi''D\bar{D}} = \Gamma_{\psi''D\bar{D}}(M^2_{\psi''})/Z_{\psi''} = 37.61$ MeV, and $\Gamma^{\rm ren}_{\psi''e^+e^-} = \Gamma_{\psi''e^+e^-}/Z_{\psi''} = 0.05181$ keV, where $Z_{\psi''} = 1 + {\rm Re}\Pi'_{\psi''}(M^2_{\psi''}) = 1.748$ and $\Gamma_{\psi''e^+e^-} = 4\pi\alpha^2 g^2_{\psi''\gamma}/(3M^3_{\psi''})$.

The obvious drawback of the considered model is the uncertain nature of the background contributions. Therefore, the validity of this model is hard to verify in other reactions. However, the model can be easily improved. It is clear that the main sources of the background in the ψ'' region are the tails from the J/ψ, $\psi(2S)$, $\psi(4040)$, $\psi(4160)$, and other resonances. The right number of resonances can be incorporated in the model by adding the corresponding pole terms to expressions (10) and (11) for $t^0_1(s)$ and $f^0_D(s)$. In that case, the parameters λ and λ_γ will effectively describe the contributions from the residual background, and it is hoped that they will be small. The $\psi(2S)$ resonance is closest to the ψ''. Its coupling to

e^+e^- is about an order of magnitude larger than that of ψ'' [28], and there are no apparent reasons for the suppression of the coupling of the $\psi(2S)$ to $D\bar{D}$. In the next subsection, we will consider in detail the model taking into account the $\psi(2S)$ resonance contribution and, in Sec. IV, discuss additional ways of checking this model.

C. The model for F_D^0 with the ψ'' and $\psi(2S)$ resonances

The connection of the $\psi(2S)$ contribution does not change the structure of expressions (6) and (7) for T_1^0 and F_D^0. Only the functions t_1^0 and f_D^0 change. Now they are given by

$$t_1^0(s) = \lambda + \frac{1}{6\pi}\frac{g^2_{\psi(2S)D\bar{D}}}{m^2_{\psi(2S)} - s} + \frac{1}{6\pi}\frac{g^2_{\psi''D\bar{D}}}{m^2_{\psi''} - s}, \tag{20}$$

$$f_D^0(s) = \lambda_\gamma + \frac{g_{\psi(2S)\gamma}g_{\psi(2S)D\bar{D}}}{m^2_{\psi(2S)} - s} + \frac{g_{\psi''\gamma}g_{\psi''D\bar{D}}}{m^2_{\psi''} - s}. \tag{21}$$

Hereinafter we use the values of $m_{\psi(2S)} = 3.6861$ GeV [28] and $\Gamma_{\psi(2S)e^+e^-} = 2.35$ keV [28]. From the relation $\Gamma_{\psi(2S)e^+e^-} = 4\pi\alpha^2 g^2_{\psi(2S)\gamma}/(3m^3_{\psi(2S)})$, we get $g_{\psi(2S)\gamma} \approx \pm 0.7262$ GeV^2. The coupling constant $g_{\psi(2S)D\bar{D}}$ is a free parameter.

Owing to the common $D^0\bar{D}^0$ and D^+D^- decay channels, the ψ'' and $\psi(2S)$ resonances can transform into each other (i.e., mix); for example, $\psi'' \to D\bar{D} \to \psi(2S)$. Therefore, it is very useful to rewrite Eqs. (6) and (7) for the amplitude T_1^0 and the form factor F_D^0 in terms which would reflect this physical aspect of the model and, in particular, introduce the amplitude describing the $\psi'' - \psi(2S)$ mixing.

Let us write the background amplitude in the form similar to Eq. (12):

$$T_{\rm bg} = \frac{e^{2i\delta_{\rm bg}(s)} - 1}{2i} = \frac{\nu(s)\lambda}{1 - i\nu(s)\lambda}. \tag{22}$$

The amplitude $T_{\rm res}$ [see Eq. (3)], corresponding to the complex of the mixed ψ'' and $\psi(2S)$ resonances, dressed by the residual background, we represent in the following symmetric form [36,42,43]:

$$T_{\rm res} = \frac{(m^2_{\psi''} - s){\rm Im}\Pi_{\psi(2S)}(s) + (m^2_{\psi(2S)} - s){\rm Im}\Pi_{\psi''}(s)}{D_{\psi''}(s)D_{\psi(2S)}(s) - \Pi^2_{\psi''\psi(2S)}(s)}, \tag{23}$$

where $D_{\psi''}(s)$ and $D_{\psi(2S)}(s)$ are the inverse propagators of ψ'' and $\psi(2S)$, respectively,

$$D_{\psi''}(s) = m^2_{\psi''} - s - \Pi_{\psi''}(s), \tag{24}$$

$$D_{\psi(2S)}(s) = m^2_{\psi(2S)} - s - \Pi_{\psi(2S)}(s), \tag{25}$$

$$\Pi_{\psi''}(s) = \frac{i}{6\pi}\frac{g^2_{\psi''D\bar{D}}}{1 - i\nu(s)\lambda}\nu(s), \tag{26}$$

$$\Pi_{\psi(2S)}(s) = \frac{i}{6\pi}\frac{g^2_{\psi(2S)D\bar{D}}}{1 - i\nu(s)\lambda}\nu(s), \tag{27}$$

and $\Pi_{\psi''\psi(2S)}(s)$ is the amplitude describing the $\psi'' - \psi(2S)$ mixing caused by the $\psi'' \to D\bar{D} \to \psi(2S)$ transitions via the real $D\bar{D}$ intermediate states,

$$\Pi_{\psi''\psi(2S)}(s) = \frac{i}{6\pi}\frac{g_{\psi''D\bar{D}}g_{\psi(2S)D\bar{D}}}{1 - i\nu(s)\lambda}\nu(s). \tag{28}$$

Note that the phase of $T_{\rm res}$ is defined by that of the denominator in Eq. (23).

For the form factor, we get

$$F_D^0(s) = e^{i\delta_{\rm bg}(s)}\frac{\mathcal{R}_{D\bar{D}}(s)}{D_{\psi''}(s)D_{\psi(2S)}(s) - \Pi^2_{\psi''\psi(2S)}(s)}, \tag{29}$$

where

$$\begin{aligned}\mathcal{R}_{D\bar{D}}(s) = {} & (m^2_{\psi''} - s)(m^2_{\psi(2S)} - s)\tilde{\lambda}_\gamma(s) \\ & + g_{\psi(2S)\gamma}[D_{\psi''}(s)\tilde{g}_{\psi(2S)D\bar{D}}(s) \\ & + \Pi_{\psi''\psi(2S)}(s)\tilde{g}_{\psi''D\bar{D}}(s)] \\ & + g_{\psi''\gamma}[D_{\psi(2S)}(s)\tilde{g}_{\psi''D\bar{D}}(s) \\ & + \Pi_{\psi''\psi(2S)}(s)\tilde{g}_{\psi(2S)D\bar{D}}(s)]\end{aligned} \tag{30}$$

and after cancellations

$$\begin{aligned}\mathcal{R}_{D\bar{D}}(s) = {} & (m^2_{\psi''} - s)(m^2_{\psi(2S)} - s)\tilde{\lambda}_\gamma(s) \\ & + (m^2_{\psi''} - s)g_{\psi(2S)\gamma}\tilde{g}_{\psi(2S)D\bar{D}}(s) \\ & + (m^2_{\psi(2S)} - s)g_{\psi''\gamma}\tilde{g}_{\psi''D\bar{D}}(s).\end{aligned} \tag{31}$$

Here $\tilde{g}_{\psi(2S)D\bar{D}}(s) = g_{\psi(2S)D\bar{D}}/|1 - i\nu(s)\lambda|$; $\tilde{g}_{\psi''D\bar{D}}(s)$ and $\tilde{\lambda}_\gamma(s)$ are given by Eqs. (17) and (19), respectively.

The curves in Fig. 5 correspond to the following values of the fitted parameters: $m_{\psi''} = 3.784$ GeV, $g_{\psi''D\bar{D}} = \pm 13.21$, $g_{\psi''\gamma} = \pm 0.2237$ GeV^2, $g_{\psi(2S)D\bar{D}} = \pm 12.91$, $\lambda = 26.89$ GeV^{-2}, and $\lambda_\gamma = \pm 2.456$ [if $\lambda_\gamma > 0 (< 0)$, then $g_{\psi''\gamma}g_{\psi''D\bar{D}} > 0 (< 0)$ and $g_{\psi(2S)\gamma}g_{\psi(2S)D\bar{D}} < 0 (> 0)$; see Eq. (31)]. Note that here $|\lambda_\gamma|$ is about an order of magnitude smaller than in the previous case, as qualitatively expected. For this fit, $\chi^2/{\rm n.d.o.f.} \approx 125/81 \approx 1.54$. The form factor has the zero at $\sqrt{s} \approx 3.816$ GeV.

Notice that the above estimates of $g_{\psi''D\bar{D}}$ and $g_{\psi(2S)D\bar{D}}$ are in agreement with the corresponding values obtained in the previous works utilizing other phenomenological approaches [24–26]. For instance, Ref. [24], from the branching ratio of $\psi'' \to D^0\bar{D}^0$, D^+D^-, gives $g_{\psi''D\bar{D}} = 12.7$, Ref. [25] has $g_{\psi''D\bar{D}} = 12.8$ and $g_{\psi(2S)D\bar{D}} = 12$, and Ref. [26] fits $g_{\psi''D\bar{D}} = 13.58 \pm 1.07$

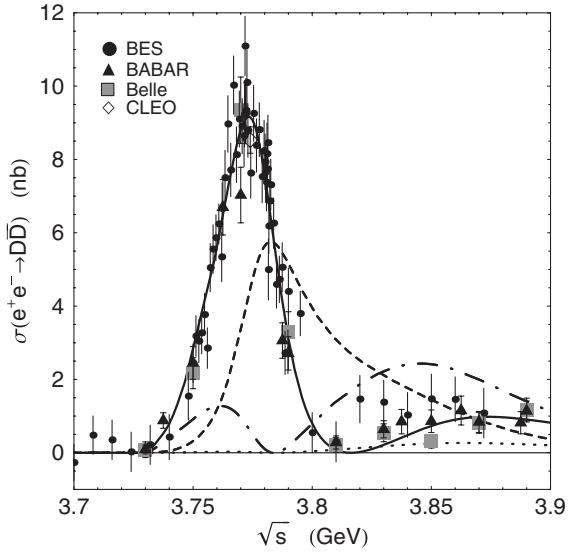

FIG. 5. The model with the ψ'' and $\psi(2S)$ resonances. The solid curve is the fit using Eqs. (5) and (29). The dashed, dot-dashed, and dotted curves show the ψ'', $\psi(2S)$, and background production contributions proportional to the coupling constants $g_{\psi''\gamma}$, $g_{\psi(2S)\gamma}$, and λ_γ in Eq. (31), respectively.

and $g_{\psi(2S)D\bar{D}} = 9.05 \pm 2.34$ from $e^+e^- \to D^0\bar{D}^0$ and $g_{\psi''D\bar{D}} = 10.71 \pm 1.75$ and $g_{\psi(2S)D\bar{D}} = 7.72 \pm 1.02$ from $e^+e^- \to D^+D^-$.

As the individual characteristics of the ψ'' resonance, one can take again the quantities dressed (renormalized) by the background contributions: $M_{\psi''} = 3.789$ GeV, $\Gamma^{\rm ren}_{\psi''D\bar{D}} = \Gamma_{\psi''D\bar{D}}(M^2_{\psi''})/Z_{\psi''} = 58.03$ MeV, and $\Gamma^{\rm ren}_{\psi''e^+e^-} = \Gamma_{\psi''e^+e^-}/Z_{\psi''} = 0.2973$ keV, where $Z_{\psi''} = 1 + {\rm Re}\Pi'_{\psi''}(M^2_{\psi''}) = 0.6905$ and $\Gamma_{\psi''e^+e^-} = 4\pi\alpha^2 g^2_{\psi''\gamma}/(3M^3_{\psi''})$. We calculated the above parameters with the use of Eqs. (12)–(17) by making the substitution

$$\lambda \to \lambda + \frac{1}{6\pi}\frac{g^2_{\psi(2S)D\bar{D}}}{m^2_{\psi(2S)} - s}; \qquad (32)$$

i.e., in the ψ'' resonance region, we included in $T_{\rm bg}$ the total background from the amplitude λ and the $\psi(2S)$ contribution and took into account in $T_{\rm res}$ the ψ'' contribution dressed by this total background. For example, at the $D\bar{D}$ threshold, $\lambda + \frac{1}{6\pi}\frac{g^2_{\psi(2S)D\bar{D}}}{m^2_{\psi(2S)} - 4m^2_D} \approx 4.38$ GeV^{-2} instead of $\lambda \approx -30.35$ GeV^{-2} in the resonance plus background model.

Thus, the fitting of the mass spectrum in $e^+e^- \to D\bar{D}$ permits us to determine the resonance and background characteristics in specific models. Nevertheless, the information only on the reactions $e^+e^- \to D\bar{D}$ is still lacking to give reliable conclusions about the separate components of the reaction amplitude. The performed analysis indicates that these components can be very different in the different models. On the other hand, it is clear that the interference pattern in the ψ'' region depends on the reaction. Therefore, to toughen the selection of the models one should compare their predictions with the experimental data on the mass spectra for several different reactions.

For example, after the fitting of the $e^+e^- \to D\bar{D}$ data we all know about $D\bar{D}$ elastic scattering in the P wave at the model level; see Fig. 6. Unfortunately, these predictions are not possible to verify. However, there are many other reactions which can be measured experimentally.

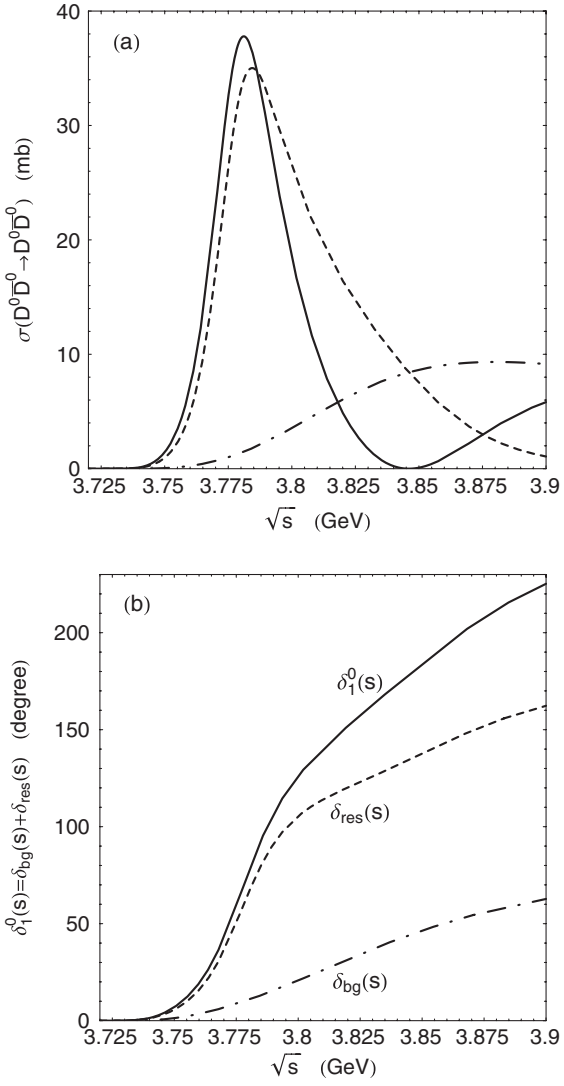

FIG. 6. The predictions of the model with the ψ'' and $\psi(2S)$ resonances. (a) The cross sections and (b) the phase shifts of $D\bar{D}$ elastic scattering in the P wave. In (a), the solid, dashed, and dot-dashed curves correspond to $\sigma(D^0\bar{D}^0 \to D^0\bar{D}^0) = 3\pi|\sin\delta^0_1(s)|^2/p^2_0(s)$, $3\pi|\sin\delta_{\rm res}(s)|^2/p^2_0(s)$, and $3\pi|\sin\delta_{\rm bg}(s)|^2/p^2_0(s)$, respectively. In particular, the model predicts that $\sigma(D^0\bar{D}^0 \to D^0\bar{D}^0) = 0 (\delta^0_1 = 180°)$ at $\sqrt{s} \approx 3.846$ GeV.

IV. THE ψ'' SHAPE IN NON-$D\bar{D}$ DECAY CHANNELS

Now we apply the last described model to construct the mass spectra in the reactions $e^+e^- \to \gamma\chi_{c0}$, $J/\psi\eta$, $\phi\eta$. In the ψ'' region, we restrict ourselves to the contributions only from the ψ'' and $\psi(2S)$ resonances, taking into account their couplings to the $\gamma\chi_{c0}$, $J/\psi\eta$, and $\phi\eta$ channels in the first order of perturbation theory.

The cross section for $e^+e^- \to ab$ ($ab = \gamma\chi_{c0}$, $J/\psi\eta$, $\phi\eta$) can be written as

$$\sigma^{ab}(s) = \frac{4\pi\alpha^2 k_{ab}^3(s)}{3s^{3/2}}|F_{ab}(s)|^2, \tag{33}$$

where $k_{ab}(s) = \sqrt{[s-(m_a+m_b)^2][s-(m_a-m_b)^2]}/(2\sqrt{s})$ and the form factor

$$F_{ab}(s) = \frac{\mathcal{R}_{ab}(s)}{D_{\psi''}(s)D_{\psi(2S)}(s) - \Pi^2_{\psi''\psi(2S)}(s)}, \tag{34}$$

where

$$\mathcal{R}_{ab}(s) = g_{\psi(2S)\gamma}[D_{\psi''}(s)g_{\psi(2S)ab} + \Pi_{\psi''\psi(2S)}(s)g_{\psi''ab}] + g_{\psi''\gamma}[D_{\psi(2S)(s)}g_{\psi''ab} + \Pi_{\psi''\psi(2S)}(s)g_{\psi(2S)ab}] \tag{35}$$

and $g_{\psi(2S)ab}$, $g_{\psi''ab}$ are the coupling constants of the $\psi(2S)$, ψ'' to the ab channel.

Table I presents information about the $\psi(2S)$ and ψ'' resonances in the $\gamma\chi_{c0}$, $J/\psi\eta$, and $\phi\eta$ decay channels [28,44–46], which we use to construct the corresponding mass spectra. The values for $g_{\psi(2S)ab}$ indicated in the table are obtained, up to the sign, from the data on the $\psi(2S) \to ab$ decay widths by the formula

$$\Gamma_{\psi(2S)ab} = \frac{g^2_{\psi(2S)ab}}{12\pi}k^3_{ab}(m^2_{\psi(2S)}). \tag{36}$$

Note that the available information about the $\psi'' \to \gamma\chi_{c0}$, $J/\psi\eta$, $\phi\eta$ decays are very poor [28]. Data on the mass spectra in these channels are still absent. The cross sections of the reactions $e^+e^- \to \gamma\chi_{c0}$, $J/\psi\eta$, $\phi\eta$ were measured by the CLEO Collaboration [44–46] at a single point in energy $\sqrt{s} = 3773$ MeV (at the supposed maximum).

TABLE I. Information about the $\psi(2S)$ and ψ'' resonances in $\gamma\chi_{c0}$, $J/\psi\eta$, and $\phi\eta$ decay channels [28,44–46] (errors <10% are not shown).

ab channel	$\gamma\chi_{c0}$	$J/\psi\eta$	$\phi\eta$
$B(\psi(2S) \to ab)$	9.68%	3.28%	$(2.8^{+1.0}_{-0.8}) \times 10^{-5}$
$\Gamma_{\psi(2S)ab}$ (keV)	29.4	10.0	$(8.5^{+3.0}_{-2.4}) \times 10^{-3}$
$g_{\psi(2S)ab}$ (GeV^{-1})	± 0.25	± 0.22	$\pm(2.7^{+0.5}_{-0.4}) \times 10^{-4}$
$\sigma(e^+e^- \to ab)$ (pb); at $\sqrt{s} = 3773$ MeV	72 ± 9	8.6 ± 3.9	3.1 ± 0.8

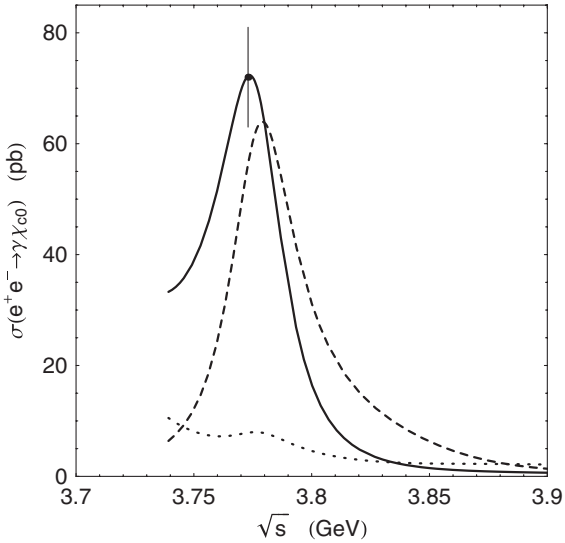

FIG. 7. The cross section for $e^+e^- \to \gamma\chi_{c0}$.

Their approximate values are presented in Table I and Figs. 7–9 by the points with the error bars. They allow us to roughly estimate the coupling constants $g_{\psi''\gamma\chi_{c0}} \approx 0.54$ GeV^{-1}, $g_{\psi''J/\psi\eta} \approx 0.053$ GeV^{-1}, and $g_{\psi''\phi\eta} \approx 1.12 \times 10^{-2}$ GeV^{-1}, by using Eqs. (33)–(35), to construct the corresponding cross sections. Here, as an illustration, we put $g_{\psi(2S)ab}$ and $g_{\psi''ab} > 0$ and $g_{\psi(2S)\gamma}/g_{\psi''\gamma} < 0$.

The solid curves in Figs. 7–9 show the $e^+e^- \to \gamma\chi_{c0}$, $J/\psi\eta$, $\phi\eta$ reaction cross sections; the dashed and dotted curves show the contributions from the ψ'' and $\psi(2S)$ resonances proportional to

$$[g_{\psi''\gamma}D_{\psi(2S)}(s) + g_{\psi(2S)\gamma}\Pi_{\psi''\psi(2S)}(s)]g_{\psi''ab}$$

and

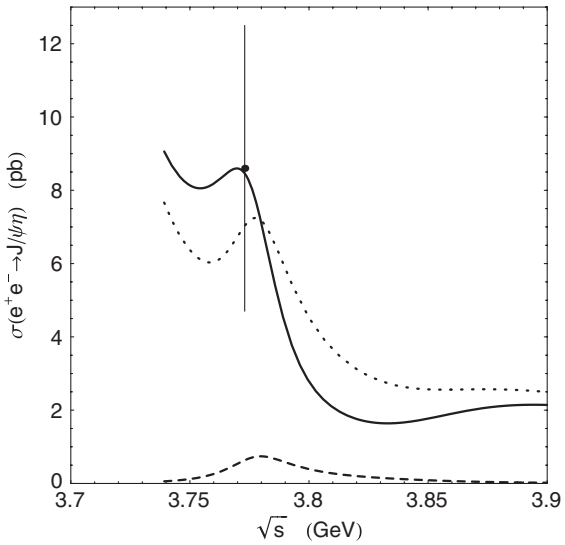

FIG. 8. The cross section for $e^+e^- \to J/\psi\eta$.

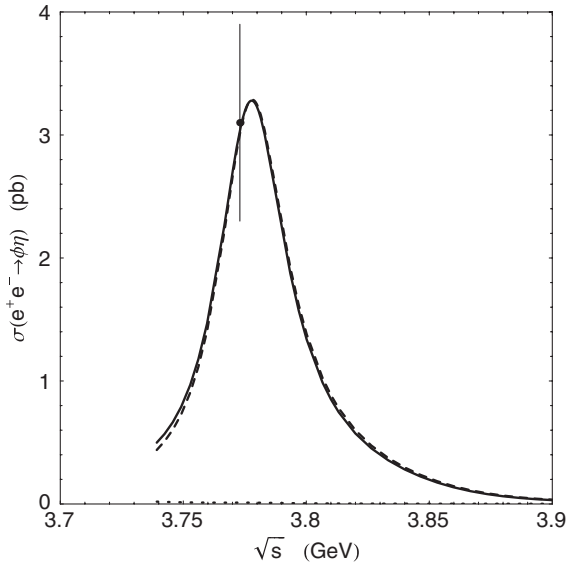

FIG. 9. The cross section for $e^+e^- \to \phi\eta$.

$$[g_{\psi(2S)\gamma}D_{\psi''}(s) + g_{\psi''\gamma}\Pi_{\psi''\psi(2S)}(s)]g_{\psi(2S)ab}$$

in Eq. (35), respectively. Note that the cross section for $e^+e^- \to \phi\eta$ is completely dominated by the ψ'' contribution.

These examples tell us that the mass spectra in the ψ'' region in the non-$D\bar{D}$ channels can be very diverse. Therefore we should expect that the data on such spectra will impose severe restrictions on the constructed dynamical models.

V. CONCLUSION

We tried to show that the shape of the ψ'' resonance keeps important information about the production mechanism and interference with background. We have considered the models satisfying the unitarity requirement and obtained good descriptions of the current data on the $e^+e^- \to D\bar{D}$ reaction cross section, in particular, in the model with the mixed ψ'' and $\psi(2S)$ resonances.

We have extracted from experiment $g^2_{\psi(2S)D\bar{D}}/(4\pi) \approx 13$.

Further improvement of the data and matching the results from the different groups on the reactions $e^+e^- \to D\bar{D}$ can result in crucial progress in understanding the complicate mechanism of the ψ'' resonance formation.

As we have shown, the measurements of the mass spectra in the ψ'' region in the non-$D\bar{D}$ channels, such as $e^+e^- \to \gamma\chi_{c0}$, $J/\psi\eta$, $\phi\eta$, etc., will also contribute to a comprehensive study of the ψ'' resonance physics and the effective selection of theoretical models.

Additional information about the ψ'' in the $D\bar{D}$ mass spectra can be extracted, for example, from weak decays $B \to \psi''K$ and photoproduction reactions at high energies $\gamma A \to \psi'' A$.

ACKNOWLEDGMENTS

This work was supported in part by RFBR, Grant No. 10-02-00016, and Interdisciplinary Project No. 102 of the Siberian division of RAS.

APPENDIX

If the parametrization of the reaction amplitude has no clear dynamical justification, it can lead to unexpected problems.

Here we comment on the ambiguity of the interfering resonances parameters determination, which has been discovered in Ref. [29] and discussed in Refs. [22,23] in connection with the ψ'' resonance parameters.

To illustrate the ambiguity of resonance parameters, we use a very simple example. Consider the model $e^+e^- \to h\bar{h}$ reaction amplitude (where h and $\bar{h}$ are hadrons) involving the resonance and background contributions [29]:

$$F(E) = \frac{A_x e^{i\varphi_x}}{M - E - i\Gamma/2} + B_x. \tag{A1}$$

Here E is the energy in the $h\bar{h}$ center-of-mass system, M is the mass and Γ the energy-independent width of the resonance, and A_x, φ_x, and B_x are the real parameters. At fixed M and Γ, there are two solutions for A_x, φ_x, and B_x [29]:

$$\text{(I)} \quad A_x = A, \qquad B_x = B, \qquad \varphi_x = \varphi, \tag{A2}$$

$$\text{(II)} \quad A_x = \sqrt{A^2 - 2AB\Gamma\sin\varphi + B^2\Gamma^2}, \qquad B_x = B,$$
$$\tan\varphi_x = -\tan\varphi + B\Gamma/(A\cos\varphi), \tag{A3}$$

which yield the same cross section as a function of energy, $\sigma(E) = |F(E)|^2$, and differ in the magnitude and phase of the resonance contribution. For example, at $M = 3.77$ GeV, $\Gamma = 0.03$ GeV, $A = 0.045$ nb$^{1/2}$ GeV, $\varphi = 0$, and $B = 1.5$ nb$^{1/2}$, solution (II) gives $A_x = \sqrt{2}A$ and $\varphi_x = \pi/4$.

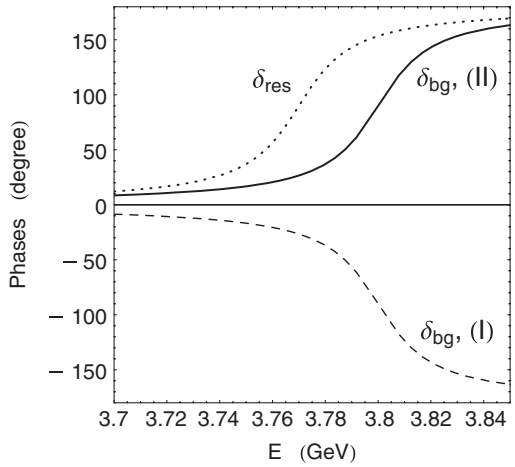

FIG. 10. The illustration of the ambiguity of the overall phase of the $e^+e^- \to h\bar{h}$ reaction amplitude defined in Eq. (A1).

For each energy, the two solutions also give the different overall phase, $\delta = \delta_{\rm res} + \delta_{\rm bg}$, of the amplitude $F(E)$. For the above numerical example, the phase $\delta_{\rm bg}$ corresponding to solutions (I) and (II) is shown in Fig. 10 by the dashed and solid curves, respectively; the phase $\delta_{\rm res} = \arctan[\frac{\Gamma}{2(M-E)}]$ is shown by the dotted curve. The origin of the rapid change of the phase $\delta_{\rm bg}$ (which is additional to $\delta_{\rm res}$) requires a special dynamical explanation (for example, the presence of extra intermediate states), for which we do not see at present any reasons.

[1] P. A. Rapidis *et al.*, Phys. Rev. Lett. **39**, 526 (1977).
[2] I. Peruzzi *et al.*, Phys. Rev. Lett. **39**, 1301 (1977).
[3] W. Bacino *et al.*, Phys. Rev. Lett. **40**, 671 (1978).
[4] R. H. Schindler *et al.*, Phys. Rev. D **21**, 2716 (1980).
[5] M. Ablikim *et al.*, Phys. Lett. B **603**, 130 (2004).
[6] M. Ablikim *et al.*, Phys. Rev. Lett. **97**, 121801 (2006).
[7] M. Ablikim *et al.*, Phys. Lett. B **641**, 145 (2006).
[8] M. Ablikim *et al.*, Phys. Rev. Lett. **97**, 262001 (2006).
[9] M. Ablikim *et al.*, Phys. Lett. B **652**, 238 (2007).
[10] M. Ablikim *et al.*, Phys. Lett. B **659**, 74 (2008).
[11] M. Ablikim *et al.*, Phys. Lett. B **660**, 315 (2008).
[12] M. Ablikim *et al.*, Phys. Rev. Lett. **101**, 102004 (2008).
[13] M. Ablikim *et al.*, Phys. Lett. B **668**, 263 (2008).
[14] D. Besson *et al.*, Phys. Rev. Lett. **96**, 092002 (2006).
[15] S. Dobbs *et al.*, Phys. Rev. D **76**, 112001 (2007).
[16] D. Besson *et al.*, Phys. Rev. Lett. **104**, 159901(E) (2010).
[17] B. Aubert *et al.*, Phys. Rev. D **76**, 111105 (2007); Report No. SLAC-PUB-12818, 2007.
[18] B. Aubert *et al.*, Phys. Rev. D **79**, 092001 (2009).
[19] G. Pakhlova *et al.*, Phys. Rev. D **77**, 011103 (2008).
[20] K. Yu. Todyshev, Proc. Sci. ICHEP2010 (2010) 218.
[21] V. V. Anashin *et al.*, Chinese Phys. C **34**, 650 (2010).
[22] K. Yu. Todyshev, in *Proceedings of the International Workshop on e^+e^- collisions from Phi to Psi, 2011, Novosibirsk*, http://phipsi11.inp.nsk.su/program.php (unpublished).
[23] V. V. Anashin *et al.*, Phys. Lett. B **711**, 292 (2012).
[24] M.-Z. Yang, Mod. Phys. Lett. A **23**, 3113 (2008).
[25] H.-B. Li, X.-S. Qin, and M.-Z. Yang, Phys. Rev. D **81**, 011501 (2010).
[26] Y.-J. Zhang and Q. Zhao, Phys. Rev. D **81**, 034011 (2010).
[27] K. Nakamura *et al.* (Particle Data Group), J. Phys. G **37**, 075021 (2010).
[28] J. Beringer *et al.* (Particle Data Group), Phys. Rev. D **86**, 010001 (2012).
[29] A. D. Bukin, arXiv:0710.5627.
[30] H. Mendez *et al.*, Phys. Rev. D **81**, 052013 (2010).
[31] H.-B. Li, in *Proceedings of 14th International Conference on Hadron Spectroscopy (hadron 2011), Munich, 2011*, edited by B. Grube, S. Paul, and N. Brambilla, econf C110613 (2011), arXiv:1108.5789.
[32] The BES Collaboration obtained also 14 values for the observed cross section $\sigma^{\rm obs}(e^+e^- \to D\bar{D})$ for 3.73 GeV$< \sqrt{s} <$ 3.80 GeV [13]. Then, the data corrected by the initial state radiation were extracted and analyzed in Ref. [25]. These data are consistent within experimental uncertainties with those used by us here.
[33] The branching ratios $\Gamma(\psi'' \to \text{light hadrons})/\Gamma^{\rm tot}_{\psi''}$ and $\Gamma(\psi'' \to D^0\bar{D}^0)/\Gamma(\psi'' \to D^+D^-)$ are a matter of intensive experimental investigations [1–27,30,31]. However, obtaining consistent results is yet to come [28].
[34] J. M. Blatt and V. F. Weisskopf, *Theoretical Nuclear Physics* (Wiley, New York, 1952).
[35] In using the r-dependent centrifugal barrier penetration factor in elementary particle physics (for example, in the case of the ρ meson [28]), one problem is overlooked. The existence of r implies that of potential (or background) scattering, which is not small at the usual value of $r \approx$ 1 fm, both in our case and in the case of the ρ meson [recall that the phase of P-wave scattering by the hard sphere of radius r is $\delta_{\rm bg} = -rp + \arctan(rp)$ [34], where p is the scattering momentum]. As is well known, in the ρ meson region, the background phase shift is negligible, and the $\pi\pi$ phase shift δ^1_1 is completely defined by the ρ resonance. Therefore, the descriptions of the hadronic resonance distributions taking into account the parameter r have a tentative character. As has been recently shown in Ref. [36], the π meson electromagnetic form factor can be excellently described without r ($r = 0$) in a wide energy region (-0.3 GeV$^2 < s < 1$ GeV^2) in the field theory approach taking into account the $\rho(770)$, $\rho(1450)$, and $\rho(1700)$ resonances. From a theoretical point of view, the r parameter does not fit into the models of Sec. III, and we did not introduce it. Furthermore, the data are not sensitive to its inclusion.
[36] N. N. Achasov and A. A. Kozhevnikov, Phys. Rev. D **83**, 113005 (2011).
[37] N. N. Achasov, S. A. Devyanin, and G. N. Shestakov, Z. Phys. C **22**, 53 (1984).
[38] We omit argument s of amplitudes and phases, where possible.
[39] Here we neglect the D meson isovector form factor. We also do not touch on the fine questions about the Coulomb corrections and isospin symmetry breaking.
[40] N. N. Achasov and G. N. Shestakov, Phys. Rev. D **49**, 5779 (1994).
[41] E. Eichten, K. Gottfried, T. Kinoshita, K. D. Lane, and T.-M. Yan, Phys. Rev. D **21**, 203 (1980).
[42] N. N. Achasov, S. A. Devyanin, and G. N. Shestakov, Phys. Lett. B **88**, 367 (1979).
[43] N. N. Achasov and G. N. Shestakov, Phys. Rev. D **58**, 054011 (1998).
[44] R. A. Briere *et al.*, Phys. Rev. D **74**, 031106(R) (2006).
[45] N. E. Adam *et al.*, Phys. Rev. Lett. **96**, 082004 (2006).
[46] G. S. Adams *et al.*, Phys. Rev. D **73**, 012002 (2006).